Response to Community Comments

Manuscript Number: **egusphere-2026-5788**

Dear Dr. Lyapustin,

Thank you for carefully reading our manuscript and providing detailed community comments. Your experience in MAIAC development and aerosol retrieval has been valuable in helping us evaluate our results comparisons, validation design, and interpretation of the results. We also thank you and your team for processing and providing the additional EPIC MAIAC results, which enable further comparisons.

We would first like to clarify the scope and objectives of our study. We fully acknowledge the contributions of the MAIAC and UV algorithm teams to aerosol remote sensing, and the value of radiative transfer and physical constraints for retrieving and interpreting aerosol properties. Our study aims to explore the potential of end-to-end learning for estimating AOD from EPIC multispectral observations and its application to aerosol monitoring at multiple times throughout the day. Once trained, the model generates AOD estimates through forward inference, offering a potential method of efficiently processing large volumes of observations. We also seek to explore the potential value of EPIC's distinctive observing configuration and spectral channels in complementing aerosol observations from polar-orbiting and geostationary satellites. The original manuscript may not explain these objectives clearly enough or adequately discuss the value of physically based methods and the respective strengths and limitations of the two approaches. In the revised version, we will describe the significance and purpose of the research more fully.

The following point-by-point response details the completed checks and supplementary analysis. We will integrate the feedback from all the public discussion and referee review into a final revision and provide the specific changes and their locations when submitting the revised manuscript. The additional figures and tables presented here support the discussion of your comments. As the integrated revision is not yet complete, final manuscript line references are not provided at this stage.

[Comment 1] Aero AOD shows a global correlation coefficient of 0.9 with AERONET for 2020 and 2023 while the EPIC UV and MAIAC perform very poorly with R=0.465 and 0.39, respectively. We published a very detailed validation analysis of MAIAC EPIC AOD in Lyapustin et al., 2021b, referenced in this manuscript. Apparently, the authors just did a formal citation without reading the paper which shows global multi-year MAIAC R=0.75-0.77. This value exceeds the real performance of Aero algorithm given by the numbers for Space- and Time-independent validation showing R=0.73-0.74. The published and presented at different science team meetings validation results for the UV algorithm from Dr. Torres are also very different from the results of this work. My question is how the authors obtained these very low R-values misrepresenting the two "physical" algorithms?

Response:

We thank Dr. Lyapustin for carefully reviewing our manuscript and pointing out the issues in Section 4.1. We also acknowledge the substantial contributions of the MAIAC and UV algorithm teams to the EPIC products.

Our intention in including the two EPIC AOD products was to assess our approach against established retrieval products. For clarity, our original processing was as follows.

For EPIC MAIAC, we used only the background-model AOD variable, AOD_551, from EPIC MAIAC and applied the scale factor supplied in the file. We retained non-fill values satisfying both Status_QA ≤ 1 and Cloud_mask $\in \{1, 7, 8, 9, 10\}$. These retained source pixels were resampled onto a 0.1° latitude–longitude grid using nearest-neighbor resampling with a 15 km radius of influence. We then extracted the output grid point for each station.

For EPIC UV, we selected the 500 nm component of FinalAerosolOpticalDepth using the Wavelength field; this corresponds to index 2. Negative AOD values were excluded, but FinalAlgorithmFlags was not applied. For each station, we selected the geographically nearest pixel using the supplied latitude and longitude, with a maximum station-to-pixel distance of 25 km. If that pixel had no valid AOD, no alternative pixel was selected.

We will remove Fig. 2g–h and any statements relying on these panel data to claim excessive superiority over existing products will be revised. We will discuss the published validation results as comparable benchmarks for our own results. We also wish to clarify that our method was evaluated using several different validation

strategies. These results support the performance of our method under the corresponding validation conditions. The MAIAC and UV products were used only for cross comparisons and did not contribute to model training, parameter selection, or the generation of application results. Therefore, removing Fig. 2(g)-(h) does not change these numerical results.

In addition, the original processing and collocation code used for EPIC MAIAC and EPIC UV comparison in the manuscript is available upon request. We would be grateful for any guidance you could offer on our use of these products. We accept that the discrepancy of our results and published validation statistics is very large to explain only by differences in collocation procedures. Therefore, we do not view the original comparison of MAIAC and UV as sufficiently reliable for quantitative assessment. Pending a complete re-analysis of our processing steps based on data provider guidance and literature, these comparisons are removed from the revised manuscript.

[Comment 2] I was surprised to see that in Figure 5 showing global AOD for August 29, 2023, the EPIC Aero algorithm is compared with MAIAC MODIS algorithm rather than with MAIAC EPIC. Our quick check showed that MAIAC data are not available for two days of 28-29 August 2023 because EPIC L1B data for these days were missing at the time of MAIAC processing. We have just processed these days. The daily-average MAIAC EPIC AOD (background model) for August 29 is displayed below for the comparison. It shows that MAIAC has more coverage than the Aero algorithm contrary to the (very strong) statement made in the paper (Ln. 201):

"Due to retrieval failures and algorithmic limitations, the numbers of valid collocated samples for the two physical algorithms (N = 198,004 and N =147,368) is substantially lower than DL method (N = 271,628)."

It also shows that in the emission source regions, MAIAC EPIC AOD is close to MAIAC MODIS AOD while the Aero AOD is significantly lower, which is admitted by the authors.

At this point I could formally ask - "why of all days in 2020 or 2023 the authors selected the day without MAIAC EPIC retrievals?" – though in combination with #1 I am beginning to doubt if I can trust presented results.

The image for August 29 also shows aerosol layer height (ALH) and spectral SSA retrieved by MAIAC EPIC v3 algorithm (referenced as Lyapustin et al., 2025). In total, MAIAC retrieves AOD, spectral imaginary refractive index and SSA, ALH, and

provides speciation of absorbing aerosols including column volume fractions and mass concentrations of BC/BrC for smoke and hematite/goethite for mineral dust.

Response:

Thank you for raising this concern, and we thank you and your team for processing and providing the EPIC MAIAC results for 29 August 2023. Your comments have made us recognize that the original manuscript did not adequately explain our intention to make the comparisons in Fig. 5. Regarding your question and our intentions, we will explain them separately below.

First, at the time Fig. 5 was prepared, we did not realize that EPIC MAIAC retrievals were unavailable for this date because the absence of MAIAC products was not part of the selection criteria examined during figure preparation. In the original manuscript, EPIC MAIAC was only used in the overall validation against collocated AERONET. Specifically, of the two study years, 2020 and 2023, we preferred the more recent year for most illustrations, while the 2020 results were primarily presented in the U.S. wildfire case in Section 5.3. Because the Canadian case in Section 5.1 already illustrated July and the Australian case in Section 5.2 illustrated October, we examined candidate dates in August and September 2023 to provide an additional example with numerous intraday observations. We selected 29 August because it contained 16 observations, has relatively extensive spatial coverage on an intraday scale, and can clearly present the results of that day. Thus, the selection was based on observation frequency and the completeness of the illustration, rather than the absence of EPIC MAIAC data.

Second, the primary purpose of Fig. 5 was to compare EPIC with a polar-orbiting satellite result and illustrate the repeated daytime observations enabled by EPIC's observing position. This comparison relates to the motivation described in the Introduction, exploring the ability for multiple daily aerosol observations using a single satellite. MODIS MAIAC was therefore selected as the cross comparison product, consistent with the reasons for comparisons in Section 5. Its widespread use and extensive evaluation in previous studies were additional reasons for choosing it as a reference.

The EPIC MAIAC results you provided enable an additional comparison using the same sensor. Our comparison with the daily mean EPIC MAIAC AOD from the background aerosol model (Fig. #2-1) shows roughly similar aerosol distributions, with high AOD within the red-boxed regions (Fig. #2-1 and Fig. #2-2). The yellow

boxes identify regions where the three results differ. Spatial coverage differs among products because of different geometries, cloud screening procedures, and retrieval validity criteria. We therefore avoid interpreting coverage differences as evidence of superior retrieval capability.

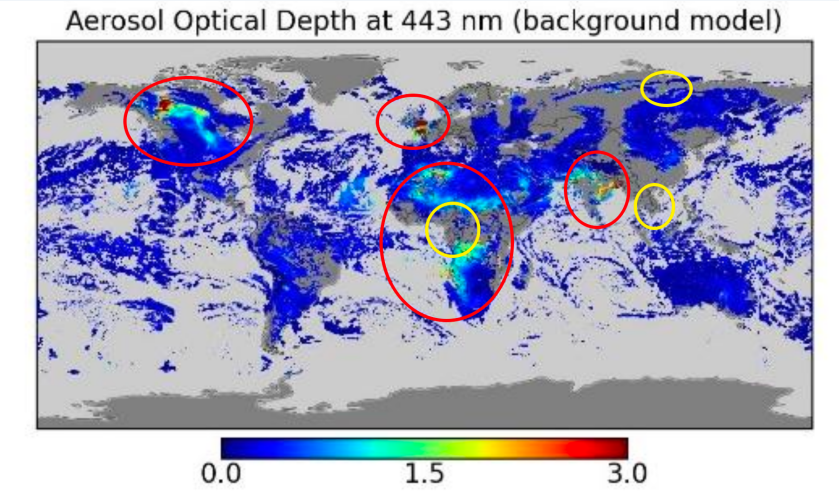


Fig. #2-1. Screenshot from comments: background model AOD (440nm)

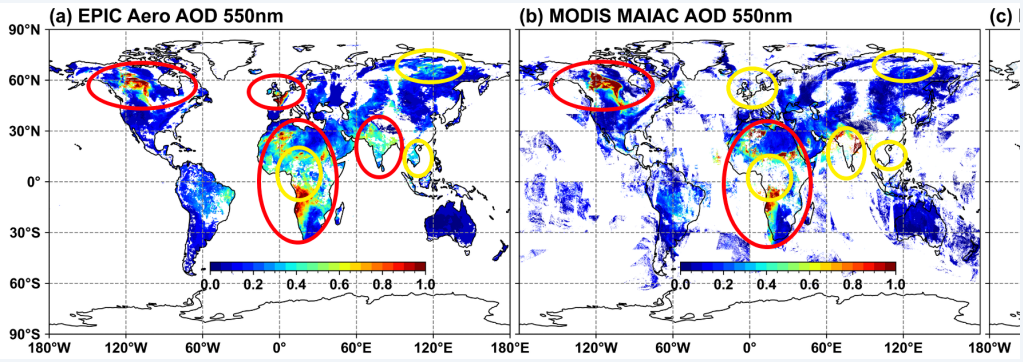


Fig. #2-2. Screenshot from the original manuscript Fig. 5.

Regarding the sentence you quoted:

"Due to retrieval failures and algorithmic limitations, the numbers of valid collocated samples for the two physical algorithms …"

We agree that this statement is not rigorous enough. We attribute it directly to retrieval failure and algorithmic limitations.

Finally, we appreciate your explanation of MAIAC's capabilities for retrieving AOD, the spectral SSA, ALH, and information on absorbing aerosol composition. These capabilities demonstrate the important value of physically based methods for the joint retrieval of multiple physically meaningful aerosol properties. Our study only achieves machine-learning-based AOD estimation and cannot replace the complete aerosol parameter system provided by MAIAC. We will describe this distinction more accurately in the Introduction and Conclusions sections and provide a more

balanced discussion of the strengths, limitations, and complementary roles of the two approaches.

[Comment 3] While the authors criticize "physical" algorithms, a knowledge of the radiative transfer and physics would benefit their research significantly. For instance, including the O2 A, B-bands or the UV bands 317, 325 nm in ML certainly reduces the accuracy of ML inference about AOD by adding unnecessary degrees of freedom uncontrolled by the ML algorithm trained on AERONET AOD. The primary use of the mentioned UV bands is for the ozone and SO2 retrieval. While there is some sensitivity to AOD, the 317, 325 nm bands have a much higher sensitivity to aerosol absorption and the height of absorbing layer because of the dominant multiple scattering. Similarly, the O2 A, B-bands depend both on AOD and ALH.

Response:

Thank you for highlighting the physical sensitivities of the O_2 A and B absorption bands and the UV channels, and the potential challenges associated with their use in machine-learning-based AOD retrieval. We agree that higher prediction skill does not imply that these channels have information specifically for AOD. Rather, they might provide indirect constraints via aerosol absorption properties, aerosol layer height, atmospheric composition, or other correlated factors. We do not intend to interpret these channels as exact AOD indicators, but to evaluate if they can improve predictive performance using an empirical retrieval framework. The original manuscript did not adequately explain the reason for including these channels, and we will address this in the revised manuscript.

Our selection of input features considered spectral information relevant to aerosol, together with environmental conditions that may affect aerosol transport, mixing, and removal. The motivation for including the UV and O_2 absorption channels is based on the assumption that they could provide useful predictive information for AOD estimation beyond the remaining inputs. Similarly, we consider that sensitivity to multiple physical factors does not preclude a net contribution to prediction skill.

We therefore supplemented the analysis with pairwise band correlations, multiple linear regression, and band ablation experiments. These analyses characterize statistical associations among the inputs, assess their linear overlap, and evaluate the effects of the selected bands on AOD prediction performance, respectively.

First, Fig. #3-1 presents the Pearson correlation matrix for the ten spectral channels, calculated using all samples. Several band pairs exhibit strong positive correlations, the coefficients for 680–688 nm, 388–443 nm, and 764–780 nm is 0.971, 0.934, and 0.851, respectively.

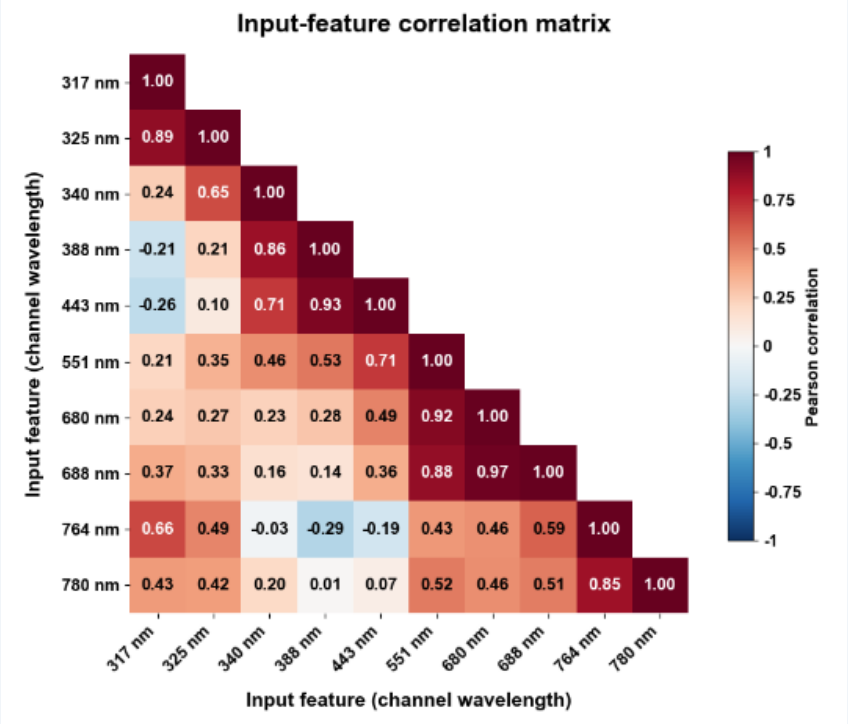


Fig. #3-1. Pearson correlation matrix of the EPIC input channels. Both axes indicate the channel wavelengths. Cell colors and annotations represent the sign and magnitude of the correlation coefficients, red indicates positive correlation, blue indicates negative correlation, and near-white colors indicate weak linear correlation.

However, pairwise correlations do not fully characterize whether a given channel can be represented by a linear combination of several other channels. We therefore fitted an ordinary least-squares regression for each UV and O_2 absorption channel, using the 443, 551, 680, and 780 nm channels as predictors:

$$B_\lambda = \beta_0 + \beta_1 B_{443} + \beta_2 B_{551} + \beta_3 B_{680} + \beta_4 B_{780} + \varepsilon$$

where B_λ is the input observation for the corresponding spectral channel. The coefficient of determination, R^2, quantifies the fraction of the target channel's variance jointly explained by the selected visible–near-infrared channels through this linear model. Accordingly, $1 - R^2$ represents the unexplained variance fraction.

As shown in Table #3-1, the degree of linear overlap differs substantially among channels. The unexplained variance fractions are 57.62%, 74.30%, and 41.45% for the 317, 325, and 340 nm channels, respectively, and 11.12% for the 764 nm channel.

In comparison, the corresponding fractions for the 388 and 688 nm channels are 7.82% and 2.97%. Thus, the variability in some channels cannot be fully represented by linear combinations of the selected visible–near-infrared observations.

Table #3-1. Multivariate linear explainability of the UV and O_2 absorption channels relative to the visible–near-infrared channels.

Target Band	Strongest Predictor Band	Max Pairwise R	R2	unexplained percent
Band 317nm	Band780nm	0.425	0.424	57.62
Band 325nm	Band780nm	0.420	0.257	74.30
Band 340nm	Band443nm	0.709	0.585	41.45
Band 388nm	Band443nm	0.934	0.922	7.82
Band 688nm	Band680nm	0.971	0.970	2.97
Band 764nm	Band780nm	0.851	0.889	11.12

To examine their predictive value, we compared three input configurations under five validation strategies: the complete feature set; the feature set excluding all UV channels; and the feature set excluding the two O_2 absorption channels. As shown in Fig. #3-2, the complete feature set generally performs better. Removing either band group generally reduces prediction performance, with the removal of the UV group having a larger overall effect than the removal of the O_2 group. Although the differences are modest, these results provide information support for the additional predictive value of retaining these band groups within the present model and validation settings.

In the revised manuscript, we will expand the discussion of the principal physical sensitivities of the UV and O_2 channels, explain the motivation for their inclusion, and present the additional analyses. We will also describe more about the characteristics and potential value of EPIC's combination of UV, visible, near-infrared, and O_2 absorption channels

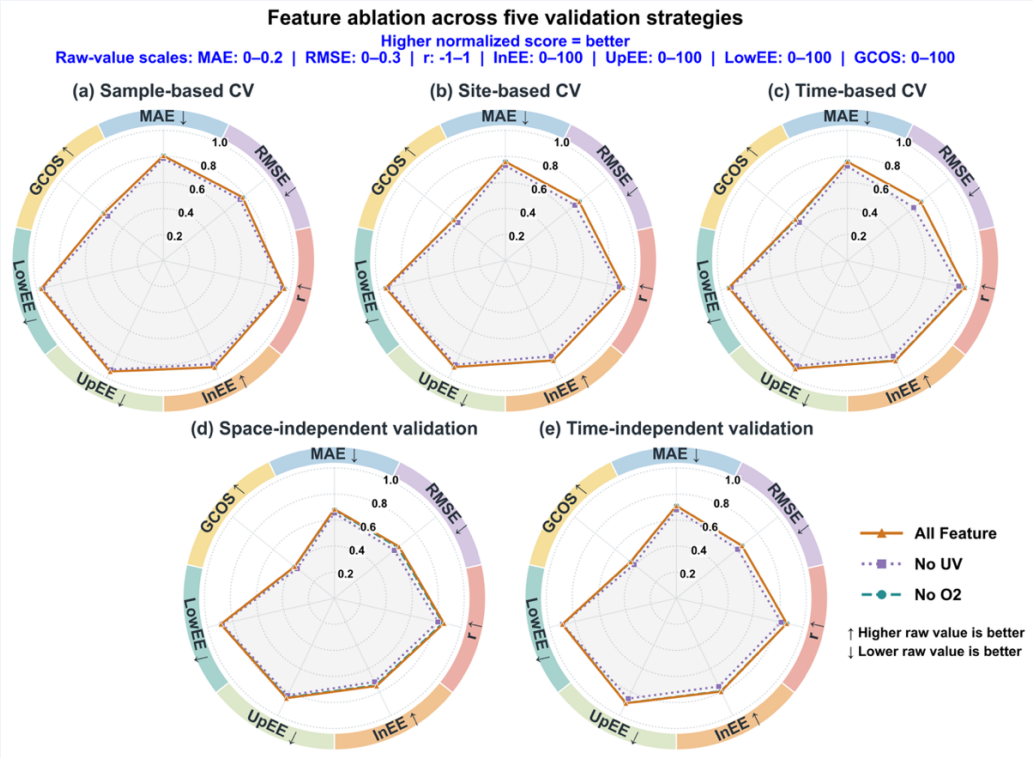


Fig. #3-2. Comparison of AOD prediction performance among three input configurations under five validation strategies: (a) sample-based cross-validation, (b) site-based cross-validation, (c) time-based cross-validation, (d) spatially independent validation, and (e) temporally independent validation. The configurations include the complete feature set (All features), exclusion of the UV channels, and exclusion of the O_2 absorption channels. The radial axes represent MAE, RMSE, r, InEE, UpEE, LowEE, and GCOS. Each metric is linearly normalized using fixed bounds, with its direction adjusted so that a larger radial score indicates better performance.

[Comment 4] Figure S7 shows a very low monthly-mean AOD both globally and regionally. For instance, the maximal monthly AOD for 2023 does not exceed 0.4 in India, and 0.3 in China and south Asia. According to Aero algorithm, these regions seemingly solved their air quality problems!

Here is a comparison of monthly Aero AOD from EPIC (top, extracted from Fig. S7) and publicly available MAIAC AOD from VIIRS (bottom) for July 2023, just one month. Aero entirely misses pollution across Europe and China, fires in Siberia (this is not surprising given lack of AERONET data to train on), and the true extent of the Canadian smoke transport over the United States.

Response:

Thank you for highlighting the low monthly AOD values in Fig. S7 and the insufficient representation of some regions with high aerosol loading. We have re-examined the monthly compositing procedure and supplemented the analysis with daily time series at six AERONET sites. During the review process, re-examination revealed that the monthly averaging procedure used in the original manuscript was not the most appropriate representation of monthly conditions and systematically reduced monthly mean values in regions where observation frequency varied strongly through time.

In the original manuscript, monthly AOD was calculated by averaging all valid retrievals within a month along the time dimension. Each valid retrieval therefore received equal weight, and days with more valid retrievals contributed more strongly to the monthly mean. For an individual grid cell, this calculation can be expressed as

$$\overline{\mathrm{AOD}} = \frac{\sum_{n_d} \mathrm{AOD}_{n_d}}{\sum_{n_d} n_d}$$

This represents the mean of all valid observations, rather than an equally weighted mean of valid daily averages. When days with more valid retrievals have lower daily mean AOD, the former is lower than the latter.

To represent the average of valid daily means, we recalculated the July 2023 composite by first averaging valid retrievals within each day and then assigning equal weight to each valid day:

$$\mathrm{AOD} = \frac{1}{D}\sum_{d} \overline{\mathrm{AOD}}_d$$

The updated July composite is shown in Fig. #4-1. Relative to the original map, the updated AeroEM composite shows more pronounced AOD enhancements over Canada and several other highlighted regions. Although the revised composite better represents several major aerosol regions, important deficiencies remain, including underestimation of some extreme pollution and wildfire events identified by the reviewer. In the Siberian–Russian Far East region marked by the yellow ellipse, AeroEM still does not reproduce the prominent high-AOD structure shown by VIIRS, although some spatial variation is evident.

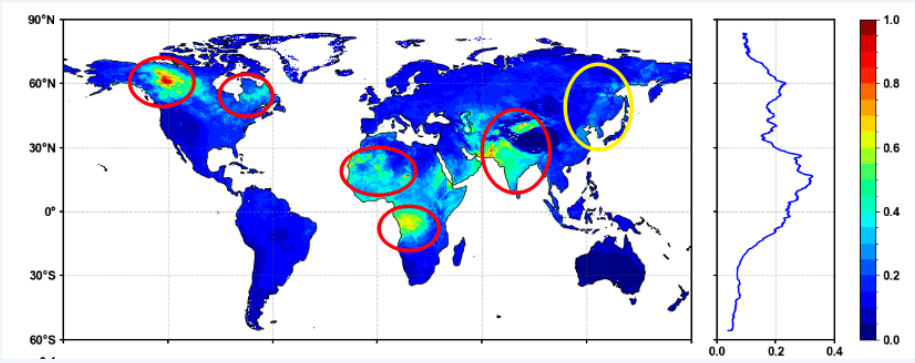


Fig. #4-1. Updated AeroEM monthly mean AOD at 550 nm for July 2023.

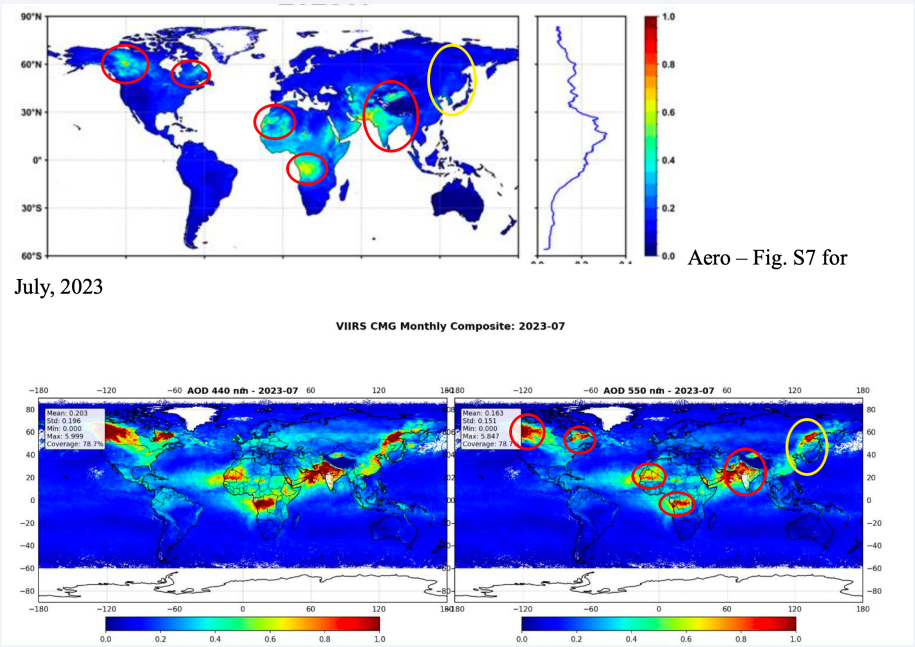


Fig. #4-2. July 2023 AOD comparison reproduced from reviewer comment #4.

To further examine regional differences and the temporal evolution of AOD, we selected six sites with available AERONET Level 2.0 observations during 2023 in a subset of the regions discussed in the comment: Beijing-CAMS, Yonsei_University, Chi_Kraeng_Station, Kanpur, Karachi, and Yellowknife_Aurora (Fig. #4-3). These comparisons provide local evidence at the selected sites.

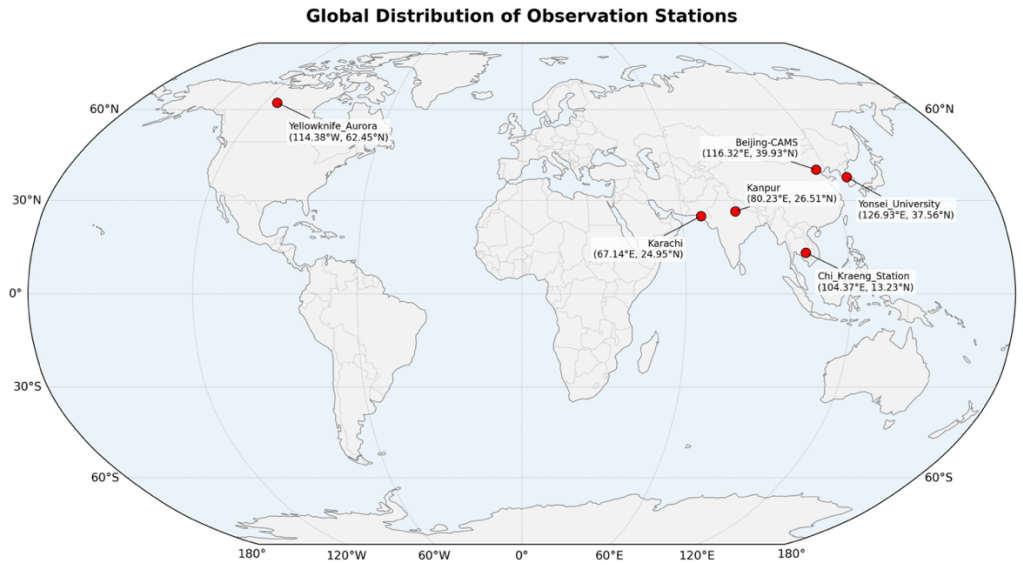


Fig #4-3. Locations of the six selected AERONET sites.

The comparisons use the VIIRS MAIAC and MODIS MAIAC. AERONET AOD was spectrally interpolated to 550 nm using its multiwavelength observations and then averaged daily; daily means were also used for AeroEM. Correlations and errors were calculated separately for each product using dates with valid observations from both that product and AERONET.

- VIIRS/NPP+JPSS Combined Aerosol Products from MAIAC Daily L3 Global at 0.05Deg CMG V002, https://doi.org/10.5067/VIIRS/VCD19A2CMG.002
- MODIS/Terra+Aqua A-OD and Water Vapor from MAIAC, Daily L3 Global 0.05Deg CMG V061, https://doi.org/10.5067/MODIS/MCD19A2CMG.061

Fig. #4-4 - Fig. #4-9 show that AeroEM reproduced broad temporal variations but underestimated the amplitudes of several high-AOD episodes. Across the six sites, correlations based on paired daily means during 2023 ranged from 0.720 to 0.890, MSE ranged from 0.0077 to 0.1096, and the number of paired days ranged from 95 to 175. At Chi_Kraeng_Station, Fig. #4-6, AeroEM achieved the highest correlation ($R = 0.890$) and lowest MSE (0.0314) among the products on their respective available paired samples, although several springtime peaks were underestimated.

The high-AOD episode at Yellowknife_Aurora during 16–26 July illustrates this limitation particularly clearly (Fig #4-9). AeroEM captured the broad enhancement and some of the associated fluctuations, but several high values were substantially lower than AERONET observations. On 17 July, AERONET AOD was approximately 3.4, compared with approximately 1.7, 3.1, and 4.0 for AeroEM, MODIS MAIAC, and VIIRS MAIAC, respectively. On 23–24 July, AERONET

AOD remained near 2.7, and both polar-orbiting MAIAC products closely represented this elevated period, whereas AeroEM yielded approximately 1.0–1.3. MODIS and VIIRS MAIAC generally represented the timing and magnitude of the major peaks more faithfully than AeroEM during this episode.

Data availability also limits some cross comparisons. AeroEM provided frequent daily values at Kanpur in July Fig #4-7, when MODIS MAIAC had no available values and VIIRS MAIAC coverage was sparse. However, greater availability does not establish greater accuracy. July AERONET observations were limited at Kanpur and Beijing-CAMS and unavailable at Karachi and Chi_Kraeng_Station, preventing direct assessment of some differences among products during this period.

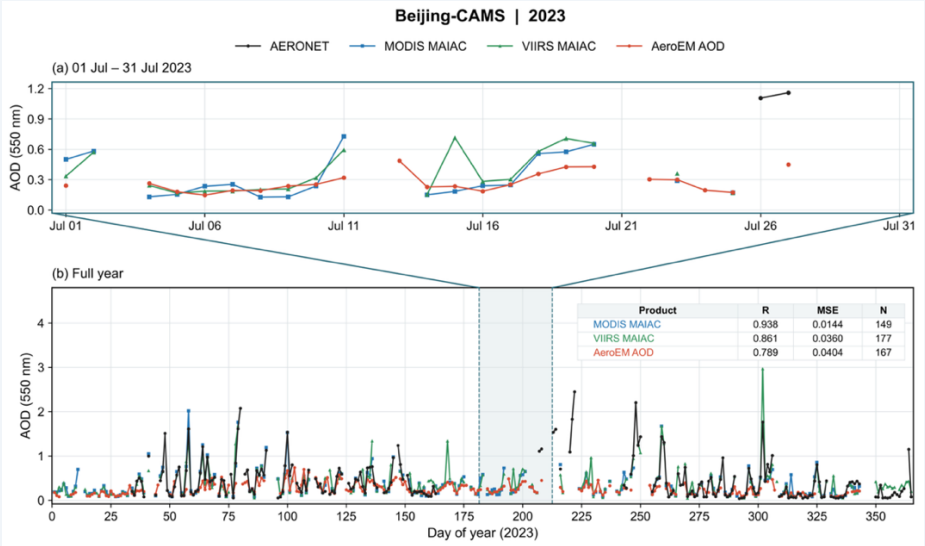


Fig. #4-4. Daily AOD at 550 nm from AERONET, MODIS MAIAC, VIIRS MAIAC, and AeroEM at Beijing-CAMS during 2023. Panel (a) shows an expanded view of 1–31 July, and panel (b) shows the full year, with July shaded.

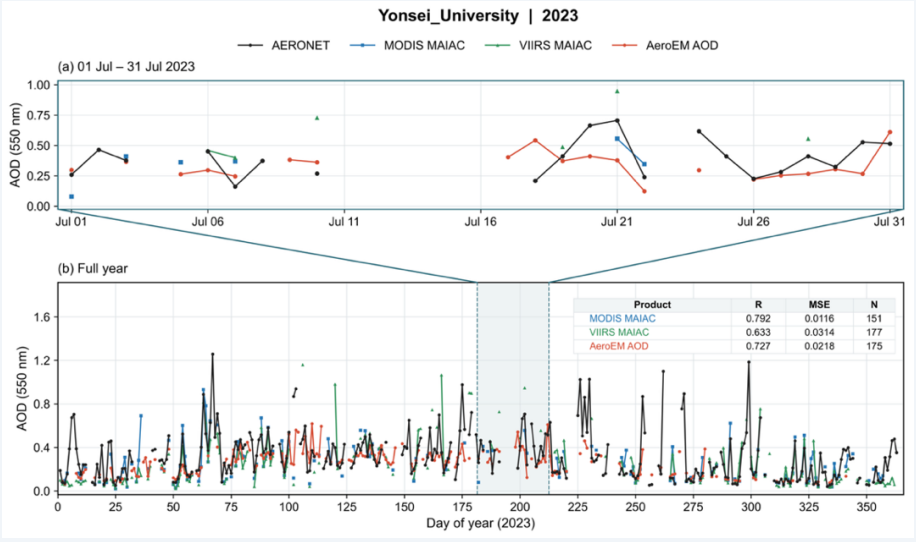


Fig. #4-5. Same as Fig. #4-4, but for Yonsei_University.

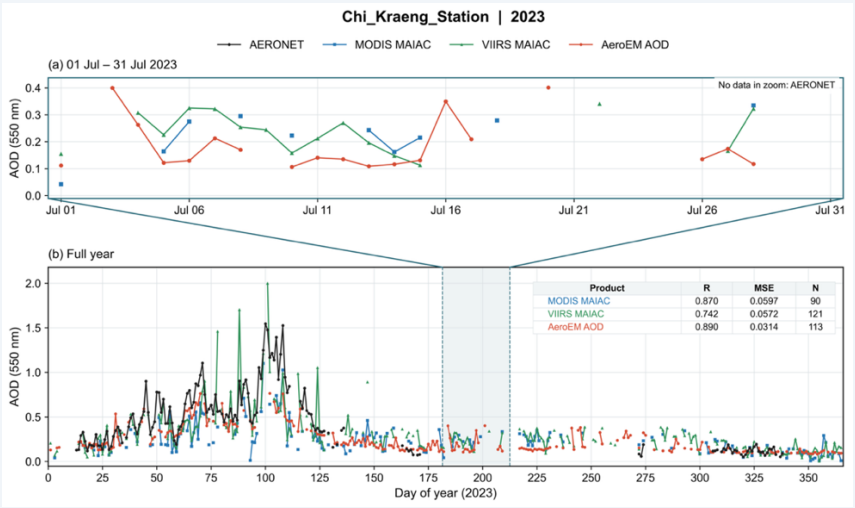


Fig. #4-6. Same as Fig. #4-4, but for Chi_Kraeng_Station. No AERONET observations are available at this site in July.

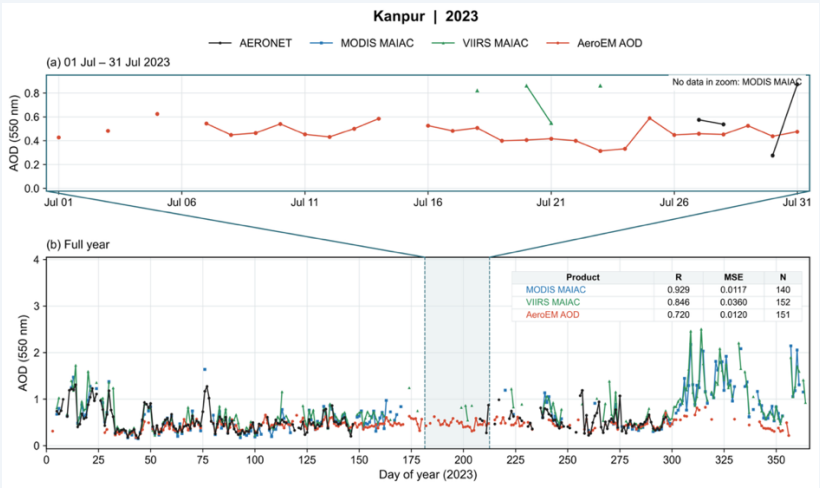


Fig. #4-7. Same as Fig. #4-4, but for Kanpur. No MODIS MAIAC values are available at this site in July, and AERONET and VIIRS MAIAC coverage is limited.

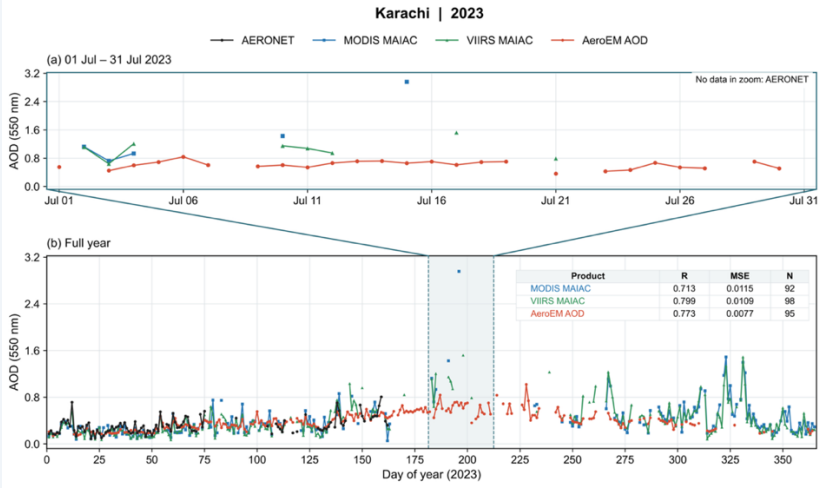


Fig. #4-8. Same as Fig. #4-4, but for Karachi. No AERONET observations are available at this site in July.

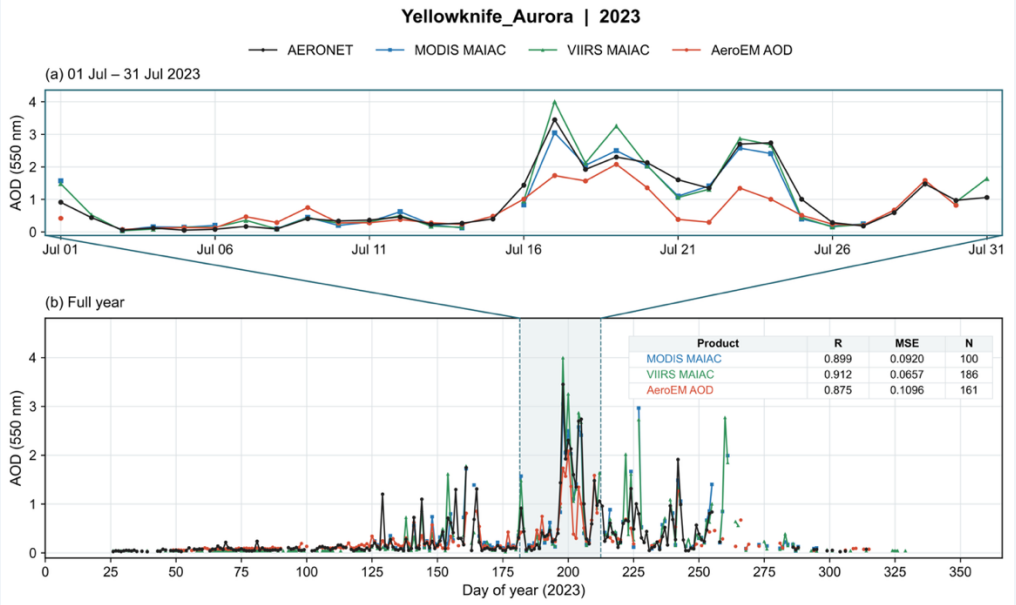


Fig. #4-9. Same as Fig. #4-4, but for Yellowknife_Aurora. The July panel illustrates the high-AOD episode and differences among products in representing its temporal evolution and magnitude.

We also provide an illustration of the spread among AeroEM ensemble predictions. AeroEM uses the mean prediction from multiple parallel MLP members as its output and stores the standard deviation among members in the AeroEM_AOD_std variable (Fig. #4-10). Figures #4-11 and #4-12 show a selected observation time on 23 July 2023 with simultaneous coverage of Canada and East Asia. In some key regions, high AOD spatially corresponds to greater ensemble spread, indicating stronger disagreement among the model members under these conditions. We interpret this standard deviation as a measure of ensemble spread and an indicator of potential uncertainty. These results suggest that the standard deviation among model-member predictions may provide useful information for guiding future model improvements. Further research could examine its relationship with actual retrieval errors and explore its potential role in uncertainty assessment and improving performance under high-AOD conditions. As this relationship has not yet been completely validated, this part will as a direction for future research in the Conclusions of the revised manuscript.

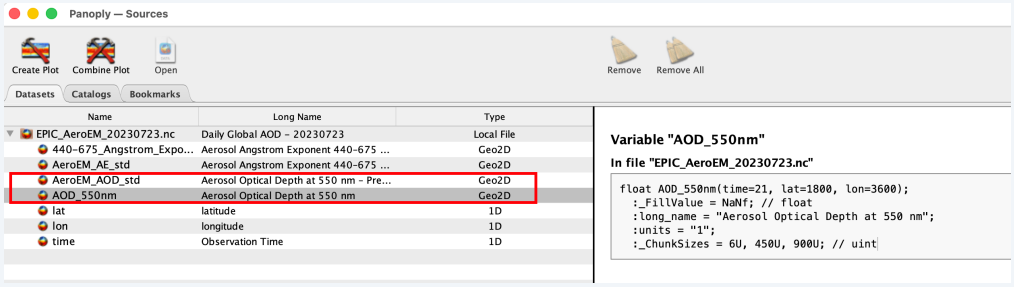


Fig. #4-10. Example data structure of the AeroEM NetCDF file for 23 July 2023. The red box identifies AOD_550nm and AeroEM_AOD_std, which store the predicted AOD at 550 nm and the standard deviation among model-member predictions, respectively.

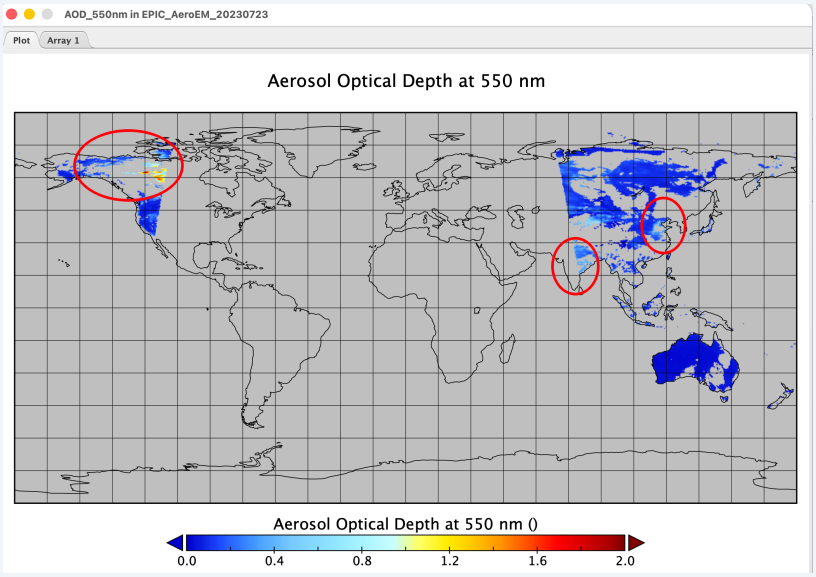


Fig. #4-11. Spatial distribution of AeroEM AOD at 550 nm at a selected observation time on 23 July 2023.

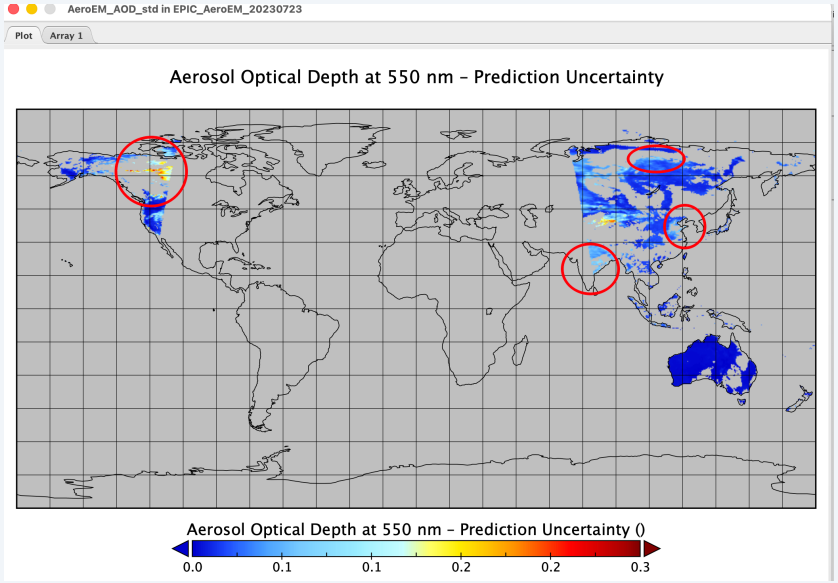


Fig. #4-12. Standard deviation among AeroEM model-member predictions, stored as AeroEM_AOD_std, at the same observation time as Fig. #4-11.